

# Label Hijacking in Track Consensus-Based Distributed Multi-Target Tracking

Helena Calatrava, Shuo Tang, Pau Closas  
Northeastern University, Boston, MA 02115, USA  
{calatrava.h, tang.shu, closas}@northeastern.edu

**Abstract**—Distributed multi-target tracking (DMTT) in limited field-of-view (FoV) sensor networks commonly suffers from *label inconsistency*, whereby different nodes disagree on the identity of the same target. Recent track-consensus DMTT (TC-DMTT) strategies mitigate this issue by enforcing kinematic and label agreement through metric-based track matching. Nevertheless, their behavior under adversarial conditions remains largely unexplored. In this paper, we reveal identity-level vulnerabilities in TC-DMTT and introduce the concept of *label hijacking*: an attack in which an adversary injects spoofed tracks to corrupt target identities across the network. Drawing on an analogy to classical pull-off deception in radar, we formalize a notion of attack stealthiness and derive an optimization-based strategy for crafting such attacks. A three-sensor network case study demonstrates the impact of the proposed attack on label consistency and tracking accuracy, showing successful target impersonation. Overall, this work highlights the need to rethink robustness at the consensus layer in DMTT frameworks.

**Index Terms**—Multi-Target Tracking, Sensor Networks, Adversarial Attack, Data Association.

## I. INTRODUCTION

Multiple target tracking (MTT) is a statistical inference problem concerned with estimating the number of physical targets present in a dynamic scene, their trajectories, and, in certain formulations, their *identities (labels)* from noisy sensor measurements [1]. Originating in the 1960s, MTT has since become a foundational technology for a wide range of perception and decision-making applications [2].

Modern MTT systems must contend with multiple sources of uncertainty beyond process and measurement noise, including time-varying target cardinality, false alarms (clutter), missed detections, target births and deaths, and data association (DA). Inspired by Mahler’s work on finite set statistics [3], random finite set (RFS) theory emerged as a mathematically elegant framework for handling these uncertainties implicitly within a unified Bayesian formulation [4], [5].

A fundamental question in MTT concerns how information should be processed in *multi-sensor settings*, where transmitting all raw measurements to a central processor is often impractical [6]. To address this, *distributed MTT (DMTT)* allows each node to perform local tracking and exchange summary information for fusion, either in the form of track-level state estimates (commonly referred to as *track-to-track fusion*) or multi-object densities. Because the RFS framework

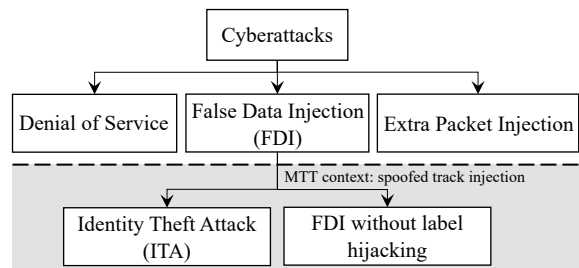


Fig. 1: Cyberattack taxonomy for distributed sensor networks [10]. We specialize false data injection to the MTT setting, focusing on identity threats.

naturally generalizes single-object distributed estimation to the multi-object case [7], a wide range of RFS-based filters, including labeled formulations [8], have been adapted to the distributed setting, predominantly relying on generalized covariance intersection (GCI) [9] for log-linear geometric averaging of probability densities.

While widely adopted, GCI-based fusion methods suffer from two key limitations. First, under *limited and non-overlapping field of view (FoV)* conditions, their performance degrades [11], and labeled formulations are prone to *label inconsistency*, whereby different nodes may assign distinct identities to the same physical target [12]. Second, more generally, density-level fusion incurs significant computational and communication overhead compared to track-to-track approaches [13]. Recent work on *track-consensus DMTT (TC-DMTT)* [14], [15] (reviewed in Sec. II) addresses these challenges through enhanced track-to-track fusion, enforcing both kinematic and label consensus using track-distance metrics, typically drawn from the optimal sub-pattern assignment (OSPA) family [16]. While effective under benign operating conditions, TC-DMTT performance in the presence of adversarial threats has received limited attention.

Although distributed architectures improve observability under limited FoV, they simultaneously expand the attack surface to cyberattacks [10] in distributed networks (see Fig. 1 for a classification). In this work, we focus on a false data injection (FDI) scenario in which an attacker injects *spoofed tracks*<sup>1</sup>, i.e., tracks that do not correspond to any true (physical) target, into the fusion process. Such attacks may arise when an adversary compromises a sensor’s communication channel and manipulates the information disseminated to other, non-

This work has been partially supported by the National Science Foundation under Awards 1845833, 2326559 and 2530870.

<sup>1</sup>Distinct from *false tracks* in the MTT literature, which arise from false alarms or data association errors.

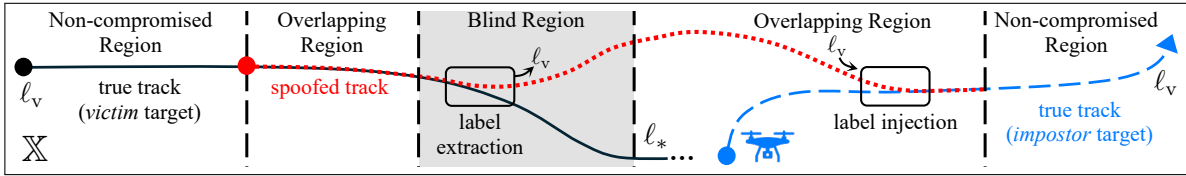


Fig. 2: We introduce *label hijacking* (extraction + injection) as the data-layer analogue of pull-off radar deception [17]. The spoofed track hijacks label  $\ell_v$  from the *victim* target, which is then tracked under an incorrect label  $\ell_*$ . After hijacking  $\ell_v$ , the spoofed track can move freely while remaining associated with that identity; by aligning with another target,  $\ell_v$  can be transferred to an *impostor* target.

compromised nodes. This renders the affected node unreliable and corrupts the distributed fusion process.

Provided that true targets remain accurately tracked, the mere presence of spoofed tracks may be tolerable in some applications. Nevertheless, a more critical failure mode arises when target identities are corrupted. As illustrated in Fig. 2, under *label hijacking*, the fusion process continues to follow a true target under incorrect labels, giving rise to what we term an *identity theft attack* (ITA) and breaking track continuity. We further show that this threat model admits a principled parallel with deception jamming in radar systems [17].

By enforcing label consensus through track-distance constraints, TC-DMTT architectures introduce identity-level vulnerabilities that remain largely unexplored. In this paper, we show that the metric-based track-matching stage constitutes a critical attack surface enabling label hijacking. Our main contributions are: (i) we introduce the track-consensus identity-theft attack (TC-ITA), which exploits this vulnerability through adversarial manipulation of track consensus; (ii) by framing TC-ITA as the data-layer analogue of classical pull-off radar deception, we define a notion of *stealthiness* and propose an model predictive control (MPC)-based strategy to generate such attacks; and (iii) we demonstrate successful identity hijacking under stealthy TC-ITA in a simulated distributed tracking scenario<sup>2</sup>.

The remainder of this paper is organized as follows. Section II reviews TC-DMTT frameworks; Section III discusses adversarial opportunities against these frameworks and introduces the proposed attack model; Section IV presents the results; and Section V concludes the paper.

## II. BACKGROUND: TRACK CONSENSUS-BASED DISTRIBUTED MULTI-TARGET TRACKING

This section reviews *track-consensus* DMTT frameworks, which we collectively refer to as *TC-DMTT*. Their distributed architecture and track-matching metrics are summarized in Secs. II-A and II-C, respectively. TC-DMTT extends classical track-to-track fusion to resolve label inconsistencies in networks with limited and non-overlapping FoVs through track consensus, as reviewed in Sec. II-B.

**Notation:** Bold symbols denote labeled quantities; uppercase symbols denote set-valued quantities. Our notation largely follows the work in [14].

### A. System Model

Fusion is performed in a fully distributed manner, without global knowledge of the network topology or FoV of other nodes. Moreover, because the fusion stage operates only on the reported track estimates and does not modify the local multi-object densities, TC-DMTT is agnostic to the specific local MTT algorithms employed at each node.

1) *Network topology:* A distributed sensor network is modeled as an undirected graph  $G = (\mathcal{N}, \mathcal{A})$ , where  $\mathcal{N}$  denotes the set of nodes and  $\mathcal{A} \subseteq \mathcal{N} \times \mathcal{N}$  the set of bidirectional communication links. Two nodes  $a, b \in \mathcal{N}$  can communicate directly if they are within communication range [10]. The neighbor set of node  $a$  is defined as  $\mathcal{N}^{(a)} \triangleq \{b \in \mathcal{N} \mid b \neq a \text{ and } (a, b) \in \mathcal{A}\}$ . Each node is equipped with a limited FoV sensor subject to false alarms and detection uncertainty, as well as local processing capabilities.

2) *Message exchange and global labeling:* At time  $k$ , each node  $a$  transmits its local labeled multi-object state estimate  $\mathbf{X}_k \subset \mathbb{X} \times \mathbb{L}$  to the other nodes, where each element  $\mathbf{x}_k = (x_k, \ell_k)$  consists of a kinematic state  $x_k \in \mathbb{X}$  and a locally unique label  $\ell_k \in \mathbb{L}$ . Since local labels are not comparable across nodes, a global labeling scheme is obtained by augmenting each label with the identity of the transmitting node, yielding  $(\ell_k, a) \in \mathbb{I} = \mathbb{L} \times \mathcal{N}$ . Each node stores the globally labeled multi-object state estimates received from each transmitting neighbor  $a$ , denoted by  $\mathbf{X}_k^{(a)} \subset \mathbb{X} \times \mathbb{I}$ .

3) *Track formation:* A *track* is a time-ordered sequence of single-object state estimates over the subset of time indices  $\mathcal{D}^{(t)} \subseteq \mathcal{K}$  at which the object is declared to exist. Each node  $a$  independently maintains a local track memory for its own estimates  $\mathbf{X}_k^{(a)}$  and for those received from its neighbors  $\{\mathbf{X}_k^{(b)}\}_{b \in \mathcal{N}^{(a)}}$ , over a finite time window  $\mathcal{K} \triangleq \{1, \dots, K\}$ . For each source  $b \in \mathcal{N}^{(a)} \cup \{a\}$ , a corresponding set of globally labeled tracks  $\mathbf{T}^{(b)} \subset \mathbb{T} \times \mathbb{I}$  is constructed by linking states that share the same global label across time.

### B. Track Consensus

Track consensus in TC-DMTT consists of two stages: (1) kinematic consensus, which aligns and fuses track states, and (2) label consensus, which propagates identity agreements across the network.

1) *Kinematic consensus:* At time  $k$ , node  $a$  has access to its own active track set  $\mathbf{T}^{(a)}$  and those from its neighbors, i.e.,  $\{\mathbf{T}^{(b)}\}_{b \in \mathcal{N}^{(a)}}$ . Here, *active* refers to tracks declared to exist and whose state estimates are available for fusion. Pairwise kinematic consensus is then performed using the two-node procedure in Fig. 3: for each neighbor  $b \in$

<sup>2</sup>Code available at <https://github.com/hcalatrava/dmtt-adversarial>

$\mathcal{N}(a)$ , node  $a$  applies this operation to the pair  $\{\mathbf{T}^{(a)}, \mathbf{T}^{(b)}\}$ , thereby producing a collection of intermediate consensus results  $\{\mathbf{X}^{(a,b,\text{con})}\}_{b \in \mathcal{N}(a)}$ . These intermediate outputs are subsequently combined sequentially to form the full (network) kinematic consensus at node  $a$ , denoted as  $\mathbf{X}^{a,\text{con}}$  (see [14], [15] for details).

We now describe the two-node (pairwise) kinematic consensus procedure between the track sets  $\mathbf{T}^{(a)}$  and  $\mathbf{T}^{(b)}$  in detail, which consists of a track-matching stage followed by kinematic fusion (Fig. 3). The role of track matching is to answer the question: *Which track in  $\mathbf{T}^{(a)}$  corresponds to which track in  $\mathbf{T}^{(b)}$ ?* First, an optimal assignment between the two track sets is computed using a track-distance metric, yielding a one-to-one matching between tracks. We review the most common choice of track metric in Sec. II-C. The resulting pairs are then filtered using a cut-off distance  $c$  (i.e., only pairs with cost below  $c$  are considered valid matches). Each matched pair is subsequently fused to produce a single track estimate, typically via a weighted combination of the individual state estimates, where the weights reflect the relative confidence of each node. Unmatched tracks may be retained according to heuristic criteria (e.g., minimum track length) [14], [15].

2) *Label consensus*: Matched tracks identified during the pairwise kinematic-consensus stage (Fig. 3) are treated as local identity agreements, and are propagated transitively through the network via a label-consensus mechanism [14], [15]. We omit the specifics of this stage, as the proposed attack induces identity corruption through compromised track matching, which is then propagated by the label consensus mechanism (see Remark 1).

### C. Track Matching Metric

Kinematic consensus requires computing distances between track sets, which in turn necessitates an appropriate track-matching metric. The works in [14], [15] adopt for this purpose the temporal extension of the OSPA metric, known as *OSPA-on-OSPA* and denoted  $\text{OSPA}^{(2)}$ . While we define both metrics below, a detailed discussion of their properties can be found in [16].

1) *OSPA*: Between two finite sets  $X, Y \in \mathcal{F}(\mathbb{X})$ , where  $\mathcal{F}(\mathbb{X})$  is the space of finite sets of  $\mathbb{X}$ ,  $X = \{x^{(1)}, \dots, x^{(m)}\}$  and  $Y = \{y^{(1)}, \dots, y^{(n)}\}$ , the  $p$ -order OSPA is defined as

$$d_p^{(c)}(X, Y) = \left( \frac{1}{n} \left( \min_{\pi \in \Pi_n} \sum_{i=1}^m d^{(c)}(x^{(i)}, y^{(\pi(i))})^p + c^p(n-m) \right) \right)^{1/p} \quad (1)$$

for  $m \leq n$ , and  $d_p^{(c)}(X, Y) \triangleq d_p^{(c)}(Y, X)$  for  $m > n$ . Here,  $\Pi_n$  denotes the set of all permutations of  $\{1, \dots, n\}$ ;  $d^{(c)}(x, y) = \min(c, d(x, y))$  denotes the truncated base distance, where  $c \in (0, \infty)$  is the cut-off parameter; and  $d(\cdot, \cdot)$  is a metric on  $\mathbb{X}$ , e.g., the Manhattan distance. Note that OSPA is defined with the conventions  $d_p^{(c)}(\emptyset, \emptyset) = 0$ , and  $d_p^{(c)}(X, Y) = c$  if one argument is empty, whereby all distances exceeding  $c$  are treated as equally large.

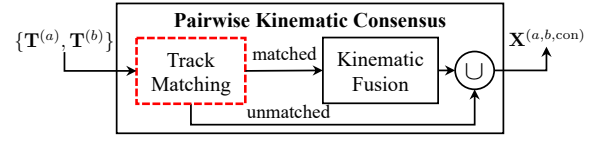


Fig. 3: Pairwise kinematic consensus between two nodes. Tracks in  $\{\mathbf{T}^{(a)}, \mathbf{T}^{(b)}\}$  are matched using a track-distance metric (Sec. II-C); matched tracks are fused and combined with retained unmatched tracks to form  $\mathbf{X}^{(a,b,\text{con})}$ . As shown in Sec. III, manipulating the track-matching stage alone is sufficient to induce *identity theft* (see Remark 1).

2) *OSPA*<sup>(2)</sup>: This metric extends OSPA to the space of finite sets of tracks  $\mathbb{T}$ , i.e.,  $\mathcal{F}(\mathbb{T})$ , as a time-averaged OSPA distance. For tracks  $t, u \in \mathbb{T}$ ,  $\text{OSPA}^{(2)}$  is given by

$$\begin{aligned} \tilde{d}^{(c)}(t, u) &= \begin{cases} \sum_{k \in \mathcal{D}^{(t)} \cup \mathcal{D}^{(u)}} \frac{d^{(c)}(\{t(k)\}, \{u(k)\})}{|\mathcal{D}^{(t)} \cup \mathcal{D}^{(u)}|}, & \text{if } \mathcal{D}^{(t)} \cup \mathcal{D}^{(u)} \neq \emptyset, \\ 0, & \text{otherwise.} \end{cases} \end{aligned} \quad (2)$$

where  $d^{(c)}(\{t(k)\}, \{u(k)\})$  is the OSPA distance between tracks evaluated at time instant  $k$ , i.e., between singleton sets, which enforces  $p = 1$ . Here, we denote by  $t(k) \in \mathbb{X}$  the single-object state of track  $t$  at time  $k \in \mathcal{D}^{(t)}$ .

## III. ADVERSARIAL MODEL

This section presents the adversarial model and feasibility assumptions for label hijacking (Sec. III-A), introduces the proposed TC-ITA strategy (Sec. III-B), and develops an MPC-based approach for generating stealthy spoofed trajectories inspired by the takeover effect in RGPO attacks (Sec. III-C) [17].

The *attack goal* is to transfer the global label of a *victim target* to a controlled *impostor target*, such that the network continues to believe it is tracking the victim while in reality following the impostor. Remarkably, if the impostor is an attacker-controlled agent (e.g., a drone), its motion can be arbitrarily designed to induce any desired behavior under the stolen identity.

**Terminology:** A *compromised node* is a sensor node whose communication channel is controlled by the attacker. A *non-compromised node* is a sensor node that is not under adversarial control; however, the attacker may intercept its transmitted messages or seek to influence its fusion output. A *blind region* is a region of the surveillance area that is not within the FoV of any non-compromised node. A *non-compromised region* is a region observed by at least one non-compromised node.

### A. Adversarial Scenario

We consider the adversarial scenario illustrated in Fig. 4, in which an attacker compromises one or more sensor nodes by gaining control over their communication channels. The attacker intercepts both the local track estimates produced at the compromised nodes and those transmitted by their non-compromised neighbors. By aggregating this information, the attacker gains access to target trajectories even outside the sensing coverage of the compromised nodes, as long as the target is observed by at least one neighbor.

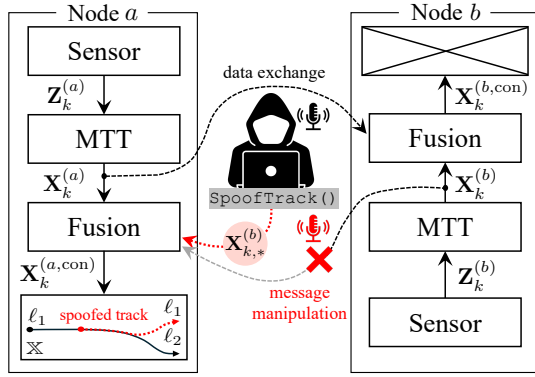


Fig. 4: False-data injection scenario in TC-DMTT (naturally extensible to larger networks). At time  $k$ , each node  $i$  forms local tracks  $\mathbf{X}_k^{(i)}$  from its measurements  $\mathbf{Z}_k^{(i)}$ . The attacker compromises node  $b$ , replaces its nominal tracks  $\mathbf{X}_k^{(b)}$  with adversarial ones  $\mathbf{X}_{k,*}^{(b)}$ , and forwards them to non-compromised neighbors, thereby corrupting their local fusion outputs  $\mathbf{X}_k^{(a,con)}$ .

From the intercepted data, the attacker constructs spoofed tracks and forwards them in place of the nominal local track estimates of the compromised nodes, thereby corrupting the local fusion processes and resulting consensus estimates of neighboring nodes. This mechanism follows the same intercept–modify–reinject paradigm as a *reply attack*.

The proposed attack is developed under the following assumptions:

- A1) Sensor nodes have limited and partially non-overlapping FoVs. This allows the victim target to enter a blind region, which is required for label extraction.
- A2) The attacker must compromise direct neighbors of the nodes whose fusion processes it seeks to manipulate and of the nodes from which it aims to intercept track information.
- A3) Since nodes lack knowledge of the network geometry, non-compromised nodes cannot verify whether a reported track is physically observed by its sending node, and therefore accept spoofed tracks as valid during consensus.
- A4) The attacker can infer when the victim target enters and exits a blind region.

The *visibility inference* in Assumption A4 enables the attacker to time the label extraction and injection stages described in Sec. III-B. It is obtained heuristically from intercepted communication patterns: the absence of reported updates over several time steps indicates that a target has left a node’s FoV, whereas continued reporting implies ongoing observability. Remarkably, the delay in detecting these transitions, which we assume to be negligible, depends on the local MTT track-management policy rather than on any knowledge of the network geometry.

### B. Identity Theft Attack Strategy

Under TC-ITA, the attacker selects a victim target tracked by the network with global label  $\ell_v$  and monitors its state estimates as reported by neighboring and compromised nodes. Let  $t_v$  and  $t_i$  denote representative victim and impostor tracks,

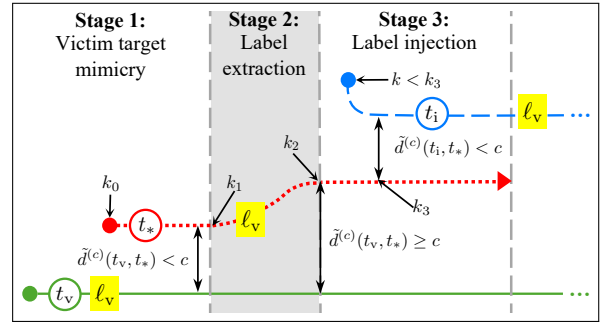


Fig. 5: Overview of the three stages of TC-ITA and the associated notation (see Sec. III-B). White and gray areas denote non-compromised and blind regions, respectively.

as reported by at least one node accessible to the attacker (compromised or non-compromised). When multiple nodes report either target, the timing and track-distance constraints introduced below are assumed to hold for all corresponding tracks. Additionally, let  $t_*$  denote the spoofed track transmitted by the attacker starting at time  $k_0$ . We now describe the three stages of TC-ITA, as depicted in Fig. 5.

1) *Victim target mimicry*:  $t_*$  assumes the victim’s global label  $\ell_v$  by *mimicking*  $t_v$  closely enough to be selected by the track-matching rule in Sec. II-B1 (see Remark 2). This requires satisfying the matching condition  $\tilde{d}^{(c)}(t_v, t_*) < c$  for some  $k \in [k_0, k_1)$ , i.e., before the victim enters the blind region. At time  $k_1$ , the attacker detects that the victim enters the blind region (Assumption A4), which triggers the start of the label extraction stage.

2) *Label extraction (pull-off stage)*: In the blind region, i.e., for  $k \in (k_1, k_2)$ , the network receives only  $t_*$  as the candidate track associated with label  $\ell_v$ . Since no competing track exists in this period,  $t_*$  can evolve arbitrarily while retaining the hijacked label. Upon the victim’s re-entry to the non-compromised region at time  $k_2$ , the separation condition  $\tilde{d}^{(c)}(t_v, t_*) \geq c$  must hold to ensure that  $t_v$  is considered a new object and therefore assigned a different label than  $\ell_v$  after confirmation; this condition must be maintained thereafter to prevent re-matching. Note that if the victim target does not re-enter the non-compromised region,  $t_*$  is not at risk of being matched with  $t_v$ , since  $\tilde{d}^{(c)}(t_v, t_*) = \tilde{d}^{(c)}(\emptyset, t_*) = c$ . Remarkably, this stage is directly analogous to a pull-off deception in radar tracking: whereas classical RGPO pulls the radar range gate away from the true target return, TC-ITA pulls off the target’s identity label. Note that label pull-off is achieved regardless of the stealthiness of  $t_*$  during the blind interval (see the hard-switch variant in Sec. IV); the stealthy variant is further inspired by the RGPO takeover regime, providing kinematic plausibility by enforcing a smooth trajectory transition.

3) *Label injection*: Assuming that the impostor target has entered the non-compromised region, the matching condition  $\tilde{d}^{(c)}(t_i, t_*) < c$  must be enforced at some time  $k_3 > k_2$ , causing  $t_i$  and  $t_*$  to be matched and thus share a global label. Since the track-matching mechanism retains the label of the longer-lived track, and assuming that the impostor target

enters the scene later than the victim, the hijacked label  $\ell_v$  is propagated to  $t_i$ . If the injection is successful, then for  $k > k_3$  the attacker can stop reporting  $t_*$ , after which  $t_i$  becomes the sole candidate associated with  $\ell_v$  and can thereafter evolve arbitrarily while retaining that identity.

**REMARK 1** (Targeted track consensus stage). *While the goal of TC-ITA is to hijack the victim target's label  $\ell_v$ , the attack does not manipulate the label-consensus mechanism itself. Instead, it operates entirely at the kinematic level by injecting a spoofed track  $t_*$  that satisfies the track-matching constraints. This causes  $t_*$  to be repeatedly matched with the victim track  $t_v$ , drift during blind intervals, and eventually match an impostor track  $t_i$ . Because label consensus is driven by persistent track matching, corrupting the kinematic consensus alone is sufficient to induce identity transfer.*

**REMARK 2** (Single-step sufficiency). *Due to the time-averaged definition in (2), a valid match between two tracks is established as soon as they are within distance  $c$  at any single time instant, irrespective of the window length. This property is exploited in the mimicry and label-injection stages of TC-ITA, where enforcing proximity for only one time step suffices to trigger track matching. During the label-extraction stage, the same property becomes critical: even a brief re-approach between the spoofed and victim tracks would immediately re-enable matching, necessitating sustained separation.*

### C. Model Predictive Control for Stealthy Attack Design

TC-ITA relies on satisfying the track-matching constraints at the transition instants shown in Fig. 5. This can be achieved through a *hard-switch strategy*, as illustrated in Fig. 6a: once the victim label has been extracted (i.e., the spoofed track has assumed  $\ell_v$ ), the attacker ceases transmission during the blind interval. When the impostor target becomes visible and is reported by non-compromised nodes, the attacker resumes transmission by forwarding a trajectory that matches the impostor track  $t_i$ . While sufficient to induce label hijacking, this strategy can produce kinematically implausible trajectories that may be detected by motion-consistency checks. To overcome this limitation, we propose a *stealthy* realization of TC-ITA that enforces kinematic consistency by enabling a smooth label pull-off, as shown in Fig. 6d. This strategy exhibits a takeover effect analogous to that observed in RGPO deception strategies [17].

Once the condition  $\tilde{d}^{(c)}(t_v, t_*) < c$  has been satisfied in the first attack stage (Sec. III-B1), the design of the spoofed track  $t_*$  must address three main objectives: (i) smoothly converging toward the impostor track  $t_i$ ; (ii) maintaining sufficient separation from the reappearing victim track  $t_v$ ; and (iii) ensuring stealth by imposing physical constraints on the planned trajectory, such as velocity and acceleration limits ( $v_{\max}$  and  $a_{\max}$ ). To systematically enforce these objectives and constraints, we formulate the design of  $t_*$  as a constrained optimal control problem and solve it via MPC, which naturally accounts for system dynamics, prediction, and physical limits in trajectory generation. We emphasize that this optimization

strategy is used *exclusively by the attacker* to generate spoofed trajectories and is not part of the tracking or fusion process.

In the following, we use the shorthand  $t(k) \triangleq x_k$  to associate any track  $t$  with its single-object kinematic state at time  $k \in \mathcal{D}^{(t)}$ . The state is defined as  $x_k = [p_k^\top, v_k^\top]^\top \in \mathbb{X}$ , where  $p_k, v_k \in \mathbb{R}^2$  denote the position and velocity vectors. This convention applies to all tracks introduced in the previous subsection, i.e.,  $t_*(k) \triangleq x_k^*$ ,  $t_i(k) \triangleq x_k^i$  and  $t_v(k) \triangleq x_k^v$ .

The spoofed state dynamics are modeled using a constant-velocity transition model, augmented with an attacker-controlled acceleration input, as

$$x_k^* = Ax_{k-1}^* + Bu_{k-1}^*, \quad (3)$$

$$A = \begin{bmatrix} 1 & 0 & \Delta t & 0 \\ 0 & 1 & 0 & \Delta t \\ 0 & 0 & 1 & 0 \\ 0 & 0 & 0 & 1 \end{bmatrix}, \quad B = \begin{bmatrix} \frac{1}{2}\Delta t^2 & 0 \\ 0 & \frac{1}{2}\Delta t^2 \\ \Delta t & 0 \\ 0 & \Delta t \end{bmatrix}, \quad (4)$$

where  $u_k^* \in \mathbb{R}^2$  is the attacker-controlled acceleration input, and  $\Delta t > 0$  denotes the sampling period.

At each time step  $k'_0$ , the attacker solves a  $K$ -step finite-horizon optimal control problem. The associated *prediction-horizon index set* is defined as

$$\mathcal{K}_{k'_0} \triangleq \{k'_0 + \kappa : \kappa = 0, 1, \dots, K\} = \{k'_0, k'_0 + 1, \dots, k'_0 + K\}, \quad (5)$$

where  $\mathcal{K}_{k'_0}^- \triangleq \mathcal{K}_{k'_0} \setminus \{k'_0 + K\}$ .

Under the initial condition  $\bar{x}_{k'_0}$ , we solve the control (acceleration) and predicted state sequences,

$$U^* \triangleq [u_k^*]_{k \in \mathcal{K}_{k'_0}^-} \in \mathbb{R}^{2 \times K}, \quad X^* \triangleq [x_k^*]_{k \in \mathcal{K}_{k'_0}} \in \mathbb{R}^{2 \times (K+1)}, \quad (6)$$

according to the optimization problem:

$$\begin{aligned} \hat{U}^*, \hat{X}^* = \arg \min_{U^*, X^*} & \alpha_p \sum_{k=k'_0+1}^{k'_0+K} \gamma_p^k \|p_k^* - p_k^i\|^2 \\ & + \alpha_v \sum_{k=k'_0+1}^{k'_0+K} \gamma_v^k \|v_k^* - v_k^i\|^2 \\ & + \alpha_c \sum_{k=k'_0+1}^{k'_0+K} \max(c - \|p_k^* - p_k^v\|, 0)^2 \end{aligned} \quad (7)$$

$$\begin{aligned} \text{s.t. } & x_k^* = Ax_{k-1}^* + Bu_{k-1}^*, \quad k \in \mathcal{K}_{k'_0} \setminus \{k'_0\}, \\ & x_{k'_0}^* = \bar{x}_{k'_0}, \\ & \|u_k^*\| \leq a_{\max}, \quad \forall k \in \mathcal{K}_{k'_0}^-, \\ & \|v_k^*\| \leq v_{\max}, \quad \forall k \in \mathcal{K}_{k'_0}. \end{aligned}$$

The first term in this objective drives the spoofed trajectory toward the impostor target, the second enforces kinematic consistency by penalizing velocity mismatch, and the third encodes the deception requirement by maintaining a minimum distance from the victim target. These terms are weighted by  $\alpha_p, \alpha_v, \alpha_c \geq 0$ , which balance the relative importance of tracking, smoothness, and separation, while  $\gamma_p, \gamma_v \in (0, 1]$  are

---

**Algorithm 1:** SpoofTrack ()

---

**Input:** Initial spoofed state  $\bar{x}_0$ , initial impostor state  $x_0^i$ , initial victim state  $x_0^v$ , prediction horizon  $K$ , attack duration  $N$ , OSPA threshold  $c$ , velocity and acceleration bounds  $v_{\max}$ ,  $a_{\max}$ .

**Output:** Spoofed state sequence  $\mathcal{S}$

**Initialization:** Record  $x_0^* \leftarrow \bar{x}_0$  in  $\mathcal{S}$ ;

**for**  $n \leftarrow 0$  **to**  $N - 1$  **do**

$(x_n^i, x_n^v) \leftarrow \text{GetFromNetwork}(n)$ ;  
     $\hat{U}^* \leftarrow \text{Solve (7) for } k'_0 \leftarrow n \text{ and parameters } \{x_n^*, x_n^i, x_n^v, K, c, a_{\max}, v_{\max}\}$ ;  
     $u_n^* \leftarrow \hat{U}^*[:, 1]$  Get first optimal control;  
     $x_{n+1}^* \leftarrow Ax_n^* + Bu_n^*$  Update spoofed state

**return**  $\mathcal{S} = [x_0^*, \dots, x_N^*]$

---

exponential discount factors that prioritize near-term deviations over those further in the prediction horizon.

Note that the same MPC structure in (7) can be used to generate the full spoofed trajectory by adapting the reference across stages: during mimicry, the reference is set to the victim state with  $\alpha_c = 0$ ; during pull-off, it is set to a prescribed *rendezvous point*; and during injection, it is set to the current impostor state.

The MPC problem in (7) is solved online at each time step by predicting the system evolution over a  $K$ -step horizon and optimizing the corresponding control sequence. Over a total duration of  $N$  time steps, the resulting online spoofed-trajectory generation strategy is summarized in Algorithm 1. At time  $k'_0$ , the current impostor and victim states,  $x_{k'_0}^i$  and  $x_{k'_0}^v$ , are obtained from the network (e.g., from compromised or non-compromised nodes accessible to the attacker). To construct the  $K$ -step trajectories required in (7), these states are then propagated forward using the assumed motion model (e.g., constant velocity), yielding auxiliary predictions that are used solely to compute the MPC solution. At the next time step  $k'_0 + 1$ , the prediction window is shifted and the process is repeated, with the initial states again refreshed from the latest network track estimates via `GetFromNetwork`.

While the trajectory-alignment terms towards  $t^i$  in (7) are convex and can be solved using standard quadratic optimization tools, the separation penalty introduces a nonconvex component. By formulating this requirement as a soft penalty, the optimization remains feasible while allowing a controlled trade-off between trajectory fidelity and separation from the true target. This is particularly important in scenarios where the spoofed and true trajectories are initially close and strict avoidance may be temporarily infeasible. In our simulations, the resulting nonlinear program is solved using *CasADi* [18].

#### IV. SIMULATION EXPERIMENTS

This section evaluates the hard-switch and stealthy TC-ITA variants introduced in Sec. III-C. We illustrate label hijacking in a representative three-node case study and assess its impact on tracking performance.

##### A. Simulation Setup

We consider a three-node distributed sensor network tracking two physical targets over a  $[-500, 2500] \text{ m} \times [0, 1000] \text{ m}$  area: a victim target, whose identity is hijacked, and an impostor target, to which the identity is transferred. The sensor nodes are located at  $[0, 0]^\top$ ,  $[1000, 0]^\top$ , and  $[1800, 0]^\top \text{ m}$  and are indexed from left to right as Nodes 1–3, with only Node 2 compromised by the attacker.

We implement the proposed TC-ITA strategy within the TC-DMTT framework of [14], which employs a local labeled multi-Bernoulli (LMB) filter at each node. A constant-velocity motion model is assumed, with process noise standard deviation  $\sigma_v = 5$  and measurement noise standard deviation  $\sigma_r = 2 \text{ m}$ . Each sensor detects objects within a relative angle of  $[-60^\circ, 60^\circ]$ , with detection probability  $P_D = 0.98$  and detection range  $r_D = 800 \text{ m}$ . Consistent with [14], the base distance metric in (2) is chosen as the Manhattan distance, i.e.,  $d(x, y) = \|x - y\|_1$ .

The target ground-truth trajectories over the evaluation window  $N = 80$  are depicted in Figs. 6a and 6d, where the physical targets  $t_v$  and  $t_i$  appear in green and blue, respectively, and the spoofed track  $t_*$  appears in red for both attacks under evaluation. The stealthy TC-ITA trajectory in Fig. 6d is generated using the MPC-based strategy summarized in Algorithm 1, with horizon  $K = 20$ , weights  $\alpha_p = 1$ ,  $\alpha_v = \alpha_c = 0.1$ , discount factors  $\gamma_p = \gamma_v = 0.99$ , and physical bounds  $v_{\max} = 30 \text{ m/s}$  and  $a_{\max} = 30 \text{ m/s}^2$ .

Figure 6 shows results for a single representative realization, while Figs. 7a and 7b report statistics averaged over  $M = 100$  Monte Carlo runs.

##### B. Label Hijacking Performance

We report local fusion (consensus) results for Node 3, i.e.,  $\hat{\mathbf{X}}_{1:N}^{(3, \text{con})}$ . This is without loss of generality, since equiprobable weights are used in the kinematic consensus stage (Sec. II-B1).

As evidenced by target and spoofed trajectories in Figs. 6a and 6d, the hard-switch attack produces an abrupt and kinematically implausible trajectory, whereas the MPC-based stealthy attack generates a smooth pull-off that closely follows the impostor target while maintaining separation from the victim, resulting in a visually plausible spoofed trajectory  $t_*$ .

The corresponding individual track streams available at Node 3 (namely its own local estimate  $\hat{\mathbf{X}}_{1:N}^{(3)}$  and those received from its neighbors  $\{\hat{\mathbf{X}}_{1:N}^{(i)}\}_{i \in \mathcal{N}(3)}$ ) are shown in Figs. 6b and 6e. These track streams constitute the inputs to the fusion stage, and show that the spoofed track  $t_*$ , injected by the compromised node (Node 2, orange), enters the fusion process as a legitimate track estimate, indistinguishable from those reported by honest nodes.

Consensus results are shown in Figs. 6c and 6f, where different colors correspond to different consensus label assignments. The victim target is initially associated with the blue label, while the impostor carries the red label; both attack variants successfully transfer the blue label to the impostor. The hard-switch strategy achieves this through an abrupt trajectory

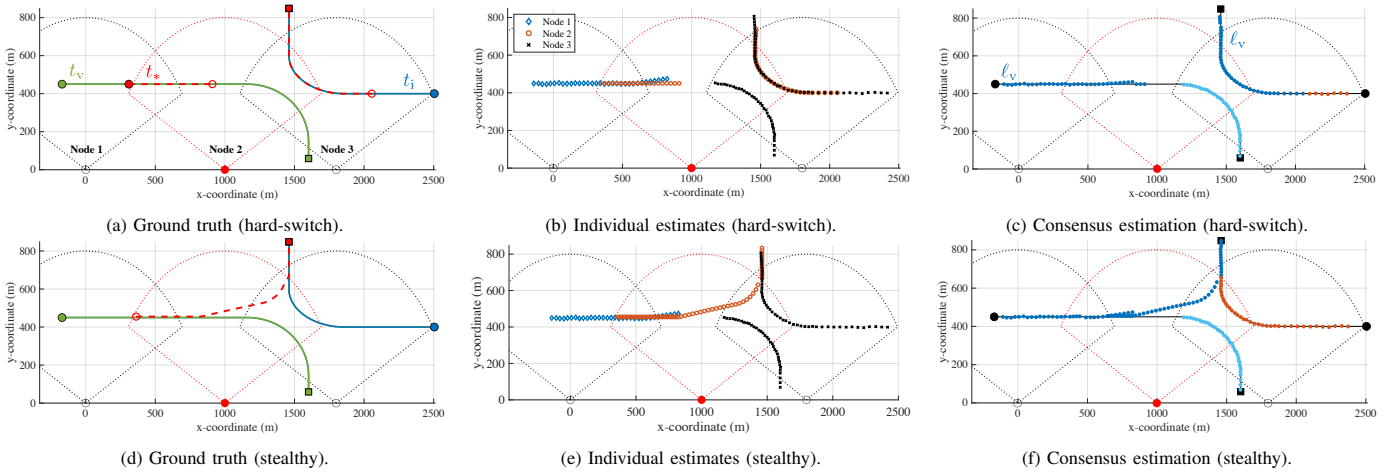


Fig. 6: Tracking results for one realization under hard-switch (top) and stealthy (bottom) TC-ITA attacks; the latter is generated via Algorithm 1. **(Left)**: Ground-truth trajectories of the victim target, the impostor target, and the spoofed trajectory. **(Middle)**: Individual track streams available at Node 3, including its own estimate and those received from neighboring nodes, which form the inputs to the fusion stage. **(Right)**: Local consensus estimate at Node 3,  $\hat{\mathbf{X}}_{1:N}^{(3, \text{con})}$ . Different colors denote different consensus label assignments; in both hard-switch and stealthy TC-ITA variants, the victim’s label  $\ell_v$  (blue) is successfully transferred to the impostor target, respectively.

transition that, while kinematically implausible, remains unmitigated by the TC-DMTT framework. This highlights that TC-DMTT frameworks rely solely on metric-based matching for label consensus, overlooking kinematic consistency as an additional integrity check. The stealthy TC-ITA further evades potential motion-consistency checks through its dynamically plausible trajectory.

Cardinality estimation results are shown in Fig. 7a. For the hard-switch attack, a transient underestimation occurs mostly during the switching interval, when the attacker ceases transmission. In contrast, under the stealthy TC-ITA, the cardinality is overestimated, as the spoofed track  $t_*$  does not necessarily coincide with any true target throughout the entire attack. Fig. 7b shows the empirical CDF (ECDF) of the instantaneous OSPA across Monte Carlo runs for hard-switch and stealthy TC-ITA, and the nominal scenario (no attack). Both attack variants significantly degrade tracking accuracy relative to the nominal case, confirming that label hijacking also impacts target tracking performance.

## V. CONCLUSION

This paper reveals identity-level vulnerabilities in track-consensus distributed multi-target tracking. By exploiting the metric-based track-matching stage, the proposed track-consensus identity-theft attack enables label hijacking and target impersonation. We introduce a hard-switch attack realization, showing that even abrupt and kinematically implausible trajectories suffice to trigger label hijacking under OSPA-based matching. We then propose a stealthy MPC-based realization that enforces smooth, physically consistent pull-off behavior while satisfying the same matching constraints. Simulations in a limited-FoV network confirm that both variants succeed. These findings highlight the need for identity-aware protection at the consensus layer.

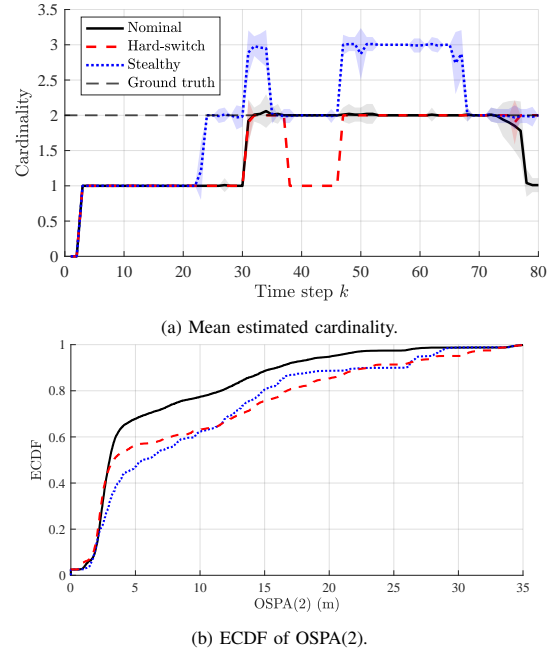


Fig. 7: Impact on tracking accuracy over the full evaluation window at Node 3 under hard-switch and stealthy TC-ITA, and no attack (nominal scenario).

## REFERENCES

- [1] Y. Bar-Shalom, P. K. Willett, and X. Tian, *Tracking and data fusion*, vol. 11. Storrs, CT, USA: YBS Publishing, 2011.
- [2] B.-N. Vo, M. Mallick, Y. Bar-Shalom, S. Coraluppi, R. Osborne, R. Mahler, and B.-T. Vo, “Multitarget tracking,” *Wiley encyclopedia of electrical and electronics engineering*, 2015.
- [3] R. P. S. Mahler, *Statistical multisource-multitarget information fusion*. Boston, MA, USA: Artech House, 2007.
- [4] B.-T. Vo, *Random Finite Sets in Multi-Object Filtering*. PhD thesis, University of Western Australia Australia, 2008.
- [5] W. Wu, H. Sun, M. Zheng, and W. Huang, *Target Tracking with Random Finite Sets*. Springer, 2023.

- [6] É. L. Souza, E. F. Nakamura, and R. W. Pazzi, "Target tracking for sensor networks: A survey," *ACM Computing Surveys (CSUR)*, vol. 49, no. 2, pp. 1–31, 2016.
- [7] R. P. Mahler, "Optimal/robust distributed data fusion: a unified approach," in *Signal Processing, Sensor Fusion, and Target Recognition IX*, vol. 4052, pp. 128–138, SPIE, 2000.
- [8] C. Fantacci, B.-N. Vo, B.-T. Vo, G. Battistelli, and L. Chisci, "Robust fusion for multisensor multiobject tracking," *IEEE Signal Processing Letters*, vol. 25, no. 5, pp. 640–644, 2018.
- [9] M. B. Hurley, "An information theoretic justification for covariance intersection and its generalization," in *Proc. of the 5th FUSION*, vol. 1, pp. 505–511, 2002.
- [10] Y. Yu and Y. Liang, "Secure multitarget tracking over decentralized sensor networks with malicious cyber attacks," *Digital Signal Processing*, vol. 117, p. 103132, 2021.
- [11] M. Üney, J. Houssineau, E. Delande, S. J. Julier, and D. E. Clark, "Fusion of finite-set distributions: Pointwise consistency and global cardinality," *IEEE Transactions on Aerospace and Electronic Systems*, vol. 55, no. 6, pp. 2759–2773, 2019.
- [12] S. Li, W. Yi, R. Hoseinnezhad, G. Battistelli, B. Wang, and L. Kong, "Robust distributed fusion with labeled random finite sets," *IEEE Transactions on Signal Processing*, vol. 66, no. 2, pp. 278–293, 2017.
- [13] L. Gao, G. Battistelli, and L. Chisci, "Event-triggered distributed multitarget tracking," *IEEE Transactions on Signal and Information Processing over Networks*, vol. 5, no. 3, pp. 570–584, 2019.
- [14] H. Van Nguyen, H. Rezafofighi, B.-N. Vo, and D. C. Ranasinghe, "Distributed multi-object tracking under limited field of view sensors," *IEEE Transactions on Signal Processing*, vol. 69, pp. 5329–5344, 2021.
- [15] J. K. Verma, J. K. Chhabra, and V. Ranga, "Track consensus-based labeled multi-target tracking in mobile distributed sensor network," *IEEE Transactions on Mobile Computing*, vol. 23, no. 6, pp. 7351–7362, 2023.
- [16] M. Beard, B. T. Vo, and B.-N. Vo, "OSPA(2): Using the OSPA metric to evaluate multi-target tracking performance," in *Proc. of the 7th ICCAIS*, pp. 86–91, 2017.
- [17] H. Calatrava, S. Tang, and P. Closas, "Advances in anti-deception jamming strategies for radar systems: A survey," *IEEE Aerospace and Electronic Systems Magazine*, pp. 1–22, 2025.
- [18] J. A. E. Andersson, J. Gillis, G. Horn, J. B. Rawlings, and M. Diehl, "CasADi – A software framework for nonlinear optimization and optimal control," *Mathematical Programming Computation*, vol. 11, no. 1, pp. 1–36, 2019.